Electronics Letters

LETTER OPEN ACCESS

Joint Noise Suppression and Resolution Enhancement of ISAR Images Using Integrated Neural Networks

Seonmin Cho[1] | Soyoon Park[1] | Youngjae Choi[2] | Seungeui Lee[2] | Youngseok Bae[3] | Seongwook Lee[1]

[1]Department of Electrical and Electronics Engineering, College of ICT Engineering, Chung-Ang University, Seoul, Republic of Korea | [2]Advanced R&D Center, Hanwha Systems, Gyeonggi-do, Republic of Korea | [3]Emerging Science and Technology Directorate, Agency for Defense Development, Daejeon, Republic of Korea

Correspondence: Seongwook Lee (seongwooklee@cau.ac.kr)

Received: 25 February 2025 | **Revised:** 29 April 2025 | **Accepted:** 7 May 2025

Funding: This work was supported by the Agency For Defense Development by the Korean Government (UG223081TD). This work was also supported by the Chung-Ang University Research Grants in 2025.

ABSTRACT

This paper proposes an integrated neural network for joint noise suppression and resolution enhancement of inverse synthetic aperture radar (ISAR) images. Unlike conventional methods that address both challenges separately, we present a unified framework that can address them simultaneously. To achieve this, we first generate a comprehensive dataset of ISAR images for various targets under different conditions using a simulation-based method. Subsequently, we develop separate generative models for noise suppression and resolution enhancement, which are then combined sequentially. This combined network uses a joint optimization strategy in training process, simultaneously updating the weights of the two networks. The proposed integrated network achieved an average peak signal-to-noise ratio and structural similarity index measure of 34.69 dB and 0.95, respectively. It demonstrates that the proposed network effectively achieves both noise suppression and resolution enhancement within a single network.

1 | Introduction

An inverse synthetic aperture radar (ISAR) is a technique that generates images of a target by using the movement of a target relative to a stationary radar platform. Unlike a conventional synthetic aperture radar that relies on the movement of the radar platform itself, ISAR is differentiated by its use of the inherent motion of the target. It has gained widespread adoption for identifying and classifying low-observable targets that are difficult to detect optically due to their distance or size, such as small aerial objects [1].

To improve target classification accuracy in ISAR systems, two key technologies have recently emerged: noise suppression and resolution enhancement. ISAR images acquired in practical environments often contain noise, which can degrade the accuracy of target identification [2]. Therefore, effective noise suppression techniques are essential for isolating the target from background noise and improving identification capabilities. Moreover, obtaining high-resolution ISAR images is crucial for detailed target analysis. Traditionally, achieving high resolution requires the use of a wide frequency bandwidth. However, it can also increase the system resource consumption and reduce operational efficiency.

Seonmin Cho and Soyoon Park contributed equally to this study.

TABLE 1 | Simulation parameters for ISAR image generation.

Parameter	Value
Operating band	X-band
Pulse repetition frequency (Hz)	10
Frequency samples	256
Observation time (s)	160
Signal-to-noise ratio (dB)	−10 to 10
Observation angle (°)	1–180

To overcome this problem, recent research has also focused on generating high-resolution ISAR images with limited frequency bandwidths, balancing image quality and resource efficiency [3].

Previous studies have typically treated noise suppression and resolution enhancement as separate problems. On the other hand, our study introduces an integrated network that simultaneously addresses both objectives to enhance overall image quality and processing efficiency. Specifically, we propose a unified network that combines distinct generative models for each task, integrating them sequentially.

2 | Simulation-Based ISAR Image Generation

Acquiring ISAR images in practical environments is often challenging due to physical limitations, such as restricted access to varied target orientations and the extensive resources required for data collection. These limitations make it difficult to obtain a diverse and comprehensive dataset. To overcome these constraints, we use a simulation-based approach for generating ISAR images. In this approach, we assume a radar platform commonly used in ISAR applications. Under this assumption, we focus on verifying the generalization performance across different targets and evaluating the robustness of the algorithm against variations in target characteristics. The simulation process consists of three steps: target modeling, electromagnetic wave modeling, and ISAR image generation. In the target modeling process, various targets such as quadcopter drones, birds, and unmanned aerial vehicles (UAVs) are represented as three-dimensional (3D) mesh structures. For target modeling, we define initial parameters such as position, velocity, and trajectory for each target and calculate the precise change in position over time. Once the target modeling is complete, we employ the physical optics (PO) method to calculate the scattered field from the modeled target [4]. The scattered field is used to model the electromagnetic waves reflected from the target, including amplitude, phase, and polarization information. Operating frequency and observation time are also considered to accurately model the received signals. Finally, we generate the ISAR image by applying a two-dimensional fast Fourier transform to the modeled signals. The specific parameters used in our simulation are shown in Table 1.

3 | Generating Dataset for Training

We generate datasets that addresses both aspects of noise suppression and resolution enhancement. First, we generate pairs

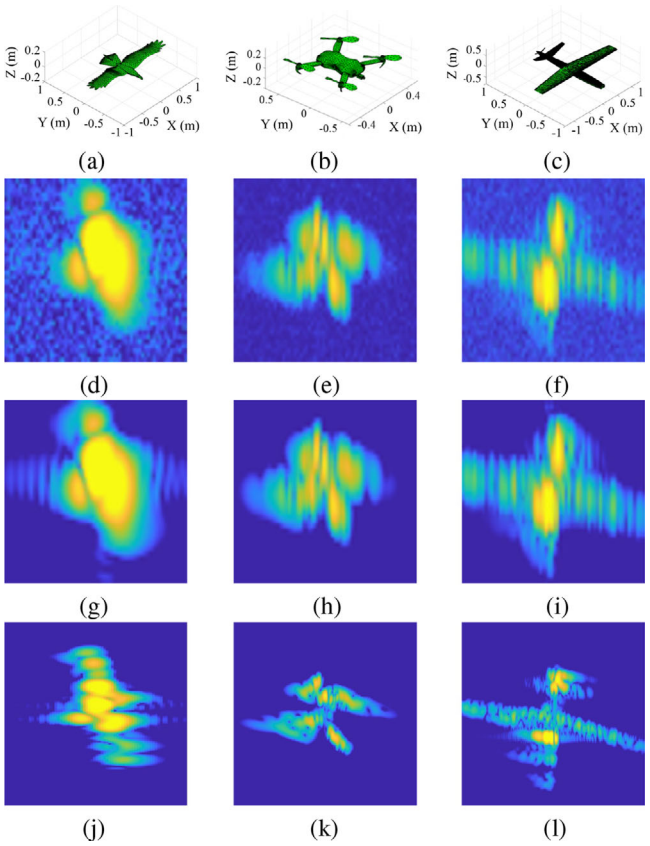

FIGURE 1 | An example of the targets and their corresponding ISAR images: (a–c) the 3D mesh-modeled targets, (d–f) the low-resolution images with noise, (g–i) the low-resolution images without noise, and (j–l) the high-resolution images without noise.

of ISAR images with and without noise. For the simulation, we use an additive white Gaussian noise to represent the background noise. Next, we generate pairs of low-resolution and high-resolution ISAR images by adjusting the bandwidth. The low-resolution images are generated using a bandwidth corresponding to 5% of the center frequency, and the high-resolution images are generated using a bandwidth corresponding to 20% of the center frequency. Through this process, we generate three types of ISAR images for each target: low-resolution images with noise, low-resolution images without bluenoise, and high-resolution images without noise. A total of 600 images are generated for each type, and examples of the generated ISAR images along with their corresponding targets are shown in Figure 1. The first, second, and third columns in Figure 1 represent the bird, drone, and UAV images, respectively. Also, the second and third rows in Figure 1 show images with noise and low-resolution, respectively. The fourth row shows the ground truth of high-resolution images without noise, which represents the ultimate objective of our proposed method for noise suppression and resolution enhancement.

4 | Network for Noise Suppression

The generator for noise suppression is designed to remove unwanted artifacts while preserving the essential features of the target image. To achieve this, our proposed architecture is

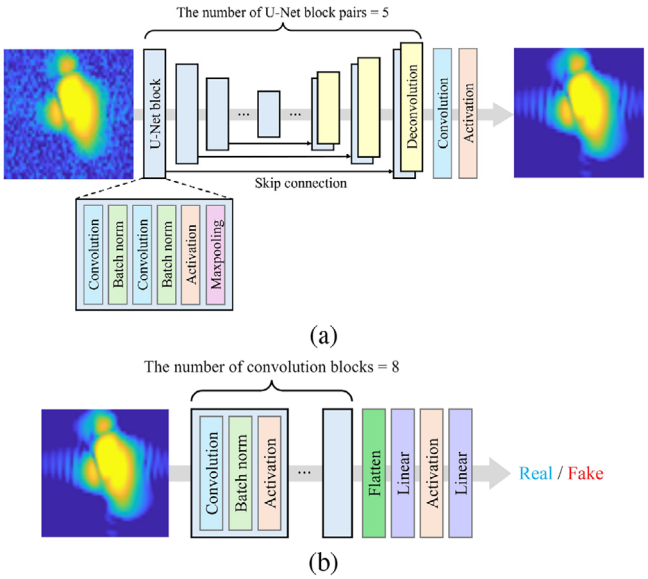

FIGURE 2 | Architecture of the proposed network for noise suppression: (a) a generator and (b) a discriminator.

based on the U-Net architecture, which follows an encoder–decoder structure. The encoder consists of two convolution layers, batch normalization, a rectified linear unit activation function, and a maxpooling layer. The sequential application of two convolutional layers enables the network to progressively extract high-level features while filtering out low-frequency components such as noise [5]. These compressed high-level features are then used to reconstruct the image during the decoding process. In this process, skip connections are used to directly transfer feature maps from the encoder to the decoder, thereby preserving the high-frequency components of the original target. Next, the structure of our discriminator consists of multiple convolutional blocks that progressively extract features from the input image. These extracted features allow the discriminator to determine whether the input is real or fake. The structures of the generator and the discriminator for noise suppression are shown in Figures 2a and 2b, respectively.

5 | Network for Resolution Enhancement

Unlike noise suppression, which preserves the original structure while removing artifacts, resolution enhancement requires transforming the input image into a new image with spatial details that are not present in the input image. It involves generating high-frequency components to reconstruct a higher resolution image. To accomplish this, our proposed architecture consists of multiple residual blocks for high-resolution feature learning, followed by several upsampling blocks to gradually increase the image size. The residual blocks add input to the output using skip connections, allowing the network to add newly generated high-resolution components to the original target data. Subsequently, the upsampling blocks physically expand the spatial dimensions of the feature maps, gradually transforming the enhanced features into a high-resolution image. The combination of residual and upsampling blocks allows for both the addition of high-resolution characteristics and gradual spatial upscaling.

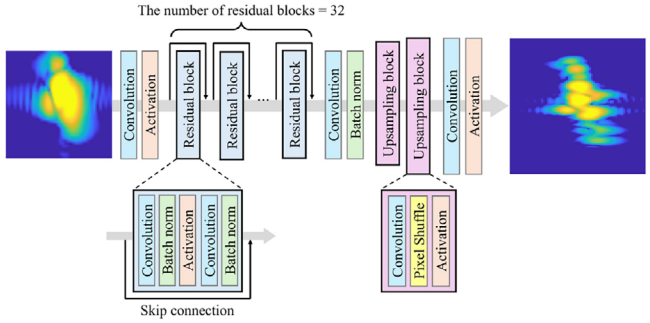

FIGURE 3 | Architecture of the proposed generator for resolution enhancement.

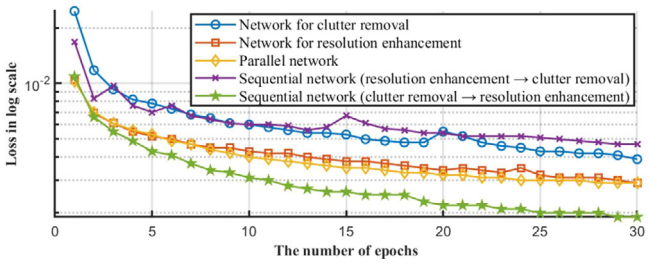

FIGURE 4 | Training loss across epochs for different generative models.

Consequently, the architecture of the proposed generator for resolution enhancement is shown in Figure 3.

6 | Proposed integrated network

After developing individual networks for noise suppression and resolution enhancement, we design an integrated neural network that achieves both objectives. When designing the integrated network, several options can be considered for combining the individual networks. In this paper, we evaluated the performance of five different combinations: two individual networks, one parallel combination, and the two serial combinations (i.e., noise suppression followed by resolution enhancement, resolution enhancement followed by noise suppression). As shown in Figure 4, the serial configuration where noise suppression precedes resolution enhancement exhibited the lowest loss value during the learning process. These results indicate that enhancing resolution before removing noise can amplify unwanted artifacts, whereas performing noise suppression first enables a more accurate reconstruction of the target object by eliminating unnecessary interference [6]. Based on this consideration, we design the integrated network by connecting the two networks in series, with noise suppression preceding resolution enhancement.

For training the integrated network, we first define the loss functions for each network. Each loss function consists of an adversarial loss and a content loss, where the content loss differs depending on the network's objective. For noise suppression, we use the mean squared error (MSE) as the content loss, while the content loss for resolution enhancement incorporates not only the MSE but also the visual geometry group (VGG) loss. The VGG loss computes the difference between the feature representations

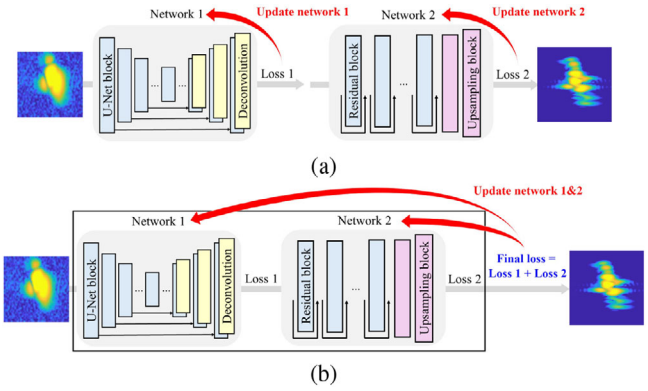

FIGURE 5 | Two different training strategies: (a) the sequential optimization and (b) the joint optimization.

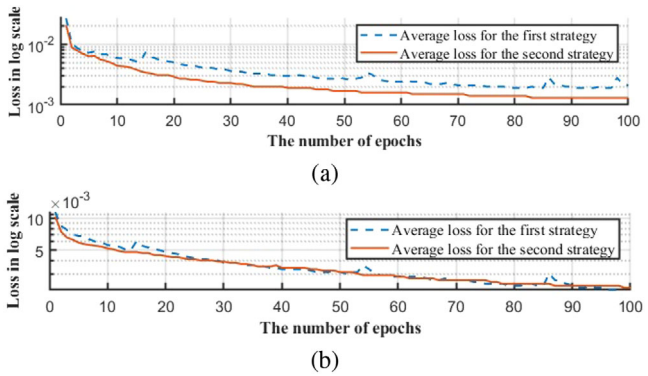

FIGURE 6 | Training loss across epochs for different training strategies: (a) the loss of first network and (b) the loss of second network.

of the generated and target images, using feature maps extracted from multiple layers of a pre-trained network. It encourages the model to focus on high-level perceptual features and textural details, resulting in images that are not only sharper but also visually realistic [7]. With these defined loss functions, we explore two different training strategies: sequential optimization and joint optimization, as shown in Figure 5. Sequential optimization involves training each network independently using its respective loss functions, after which the networks are connected in series. It allows each network to maintain optimal performance for its specific task [8]. In contrast, joint optimization combines the loss functions from both networks into a single unified loss function, thereby allowing for the simultaneous training of both networks. It enables mutual adaptation to each other's output during training, potentially improving the overall performance of the integrated network [9].

To determine the most effective approach, we implemented and evaluated both strategies. As shown in Figure 6, while both strategies achieved similar loss values for the second network (i.e., resolution enhancement), the joint optimization strategy achieved lower loss for the first network (i.e., noise suppression). Considering these results, we adopt the joint optimization strategy for our final model. Furthermore, we optimize the generator architecture by analyzing the loss with respect to the number of layers in each network. The first network achieved the lowest loss value with 5 U-Net block pairs, and the second network

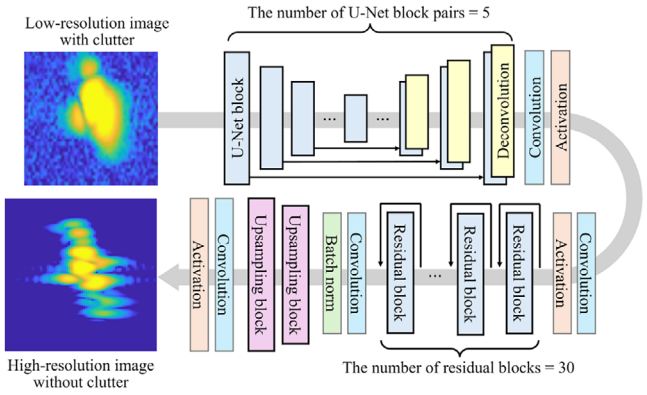

FIGURE 7 | Generator structure of the integrated network.

showed similar loss values for configurations with 30 or more residual blocks. Based on these findings, the proposed generator architecture of our integrated network is shown in Figure 7.

7 | Performance Evaluation

The training parameters for the integrated network are as follows: a batch size of 8, adaptive moment estimation as the optimizer, a learning rate of 0.0002, and a total of 100 epochs we performed a quantitative evaluation of the generated images using the peak signal-to-noise ratio (PSNR) and the structural similarity index measure (SSIM). The PSNR and SSIM metrics for the sequential strategy were 29.65 dB and 0.72, respectively, while the joint optimization strategy achieved 34.69 dB and 0.95. It demonstrated that the joint optimization strategy outperforms the sequential strategy. The joint optimization approach shows higher average PSNR and SSIM values compared to the sequential approach. Also, Figure 8 presents the qualitative results of the integrated network using the joint optimization strategy. The first, second, and third columns in Figure 8 show the input test images, the generated image with noise suppression and resolution enhancement, and the ground truth images, respectively. It demonstrated that our proposed integrated network effectively achieved both goals of noise suppression and resolution enhancement simultaneously.

8 | Conclusion

In this paper, we proposed an integrated neural network to simultaneously address noise suppression and resolution enhancement of ISAR images. Among various combination methods including parallel and serial architectures, we found that a sequential approach of noise suppression followed by resolution enhancement achieved the lowest loss. Furthermore, within the serial combination framework, we considered both a sequential optimization strategy and a joint optimization strategy during the training process. The performance of the proposed network was evaluated using a comprehensive dataset generated through simulations. The PSNR and SSIM values for the sequential optimization strategy were 29.65 dB and 0.72, respectively, while the joint optimization strategy achieved improved values of 34.69 dB and 0.95. It demonstrated that by using a joint optimization strategy in a serially connected network architecture, the proposed

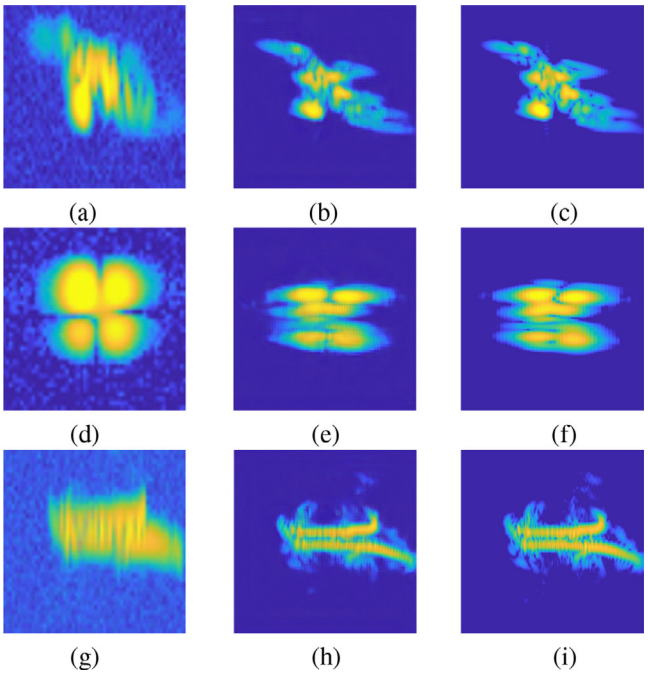

FIGURE 8 | Joint noise suppression and resolution enhancement results for each target: (a–c) a bird, (d–f) a drone, and (g–i) an UAV.

integrated network successfully addressed both noise suppression and resolution enhancement within a single pipeline.

Author Contributions

Seonmin Cho: conceptualization, methodology. **Soyoon Park:** data curation, methodology. **Youngjae Choi:** project administration. **Seungeui Lee:** project administration. **Youngseok Bae:** funding acquisition, project administration. **Seongwook Lee:** conceptualization, funding acquisition, investigation, methodology, project administration.

Acknowledgments

This work was supported by the Agency For Defense Development by the Korean Government (UG223081TD). This work was also supported by the Chung-Ang University Research Grants in 2025.

Conflicts of Interest

The authors declare no conflicts of interest.

Data Availability Statement

Research data are not shared.

References

1. W. Zhao, A. Heng, and L. Rosenberg, et al., "ISAR Ship Classification Using Transfer Learning," in *Proceedings of the 2022 IEEE Radar Conference (RadarConf'22)* (IEEE, 2022), 1–6.

2. J. Mitchell and S. Tjuatja, "ISAR Objects Embedded in Clutter Using Compressive Sensing," in *Proceedings of the 2018 IEEE International Geoscience and Remote Sensing Symposium (IGARSS 2018)* (IEEE, 2018), 4587–4590.

3. L. Zhang, M. Xing, C.-W. Qiu, J. Li, and Z. Bao, "Achieving Higher Resolution ISAR Imaging With Limited Pulses via Compressed Sampling," *IEEE Geoscience and Remote Sensing Letters* 6, no. 3 (2009): 567–571.

4. M. A. Shah, C. Tokgoz, and B. A. Salau, "Radar Cross Section Prediction Using Iterative Physical Optics With Physical Theory of Diffraction," *IEEE Transactions on Antennas and Propagation* 70, no. 6 (2022): 4683–4690.

5. M. Tabassian, X. Hu, B. Chakraborty, and J. Dh́ooge, "Clutter Filtering Using a 3D Deep Convolutional Neural Network," in *Proceedings of the 2019 IEEE International Ultrasonics Symposium (IUS)* (IEEE, 2019), 2114–2117.

6. W. Yang, Y. Yuan, W. Ren, et al., "Advancing Image Understanding in Poor Visibility Environments: A Collective Benchmark Study," *IEEE Transactions on Image Processing* 29 (2020): 5737–5752.

7. X. Sun, Z. Zhao, S. Zhang, J. Liu, X. Yang, and C. Zhou, "Image Super-Resolution Reconstruction Using Generative Adversarial Networks Based on Wide-Channel Activation," *IEEE Access* 8 (2020): 33838–33854.

8. B. Yuan, C. R. Wolfe, C. Dun, Y. Tang, A. Kyrillidis, and C. M. Jermaine, "Distributed Learning of Fully Connected Neural Networks Using Independent Subnet Training," *Proceedings of the VLDB Endowment* 15, no. 8 (2022): 1581–1590.

9. S. J. Mousavirad, D. Oliva, S. Hinojosa, and G. Schaefer, "Differential Evolution-Based Neural Network Training Incorporating a Centroid-Based Strategy and Dynamic Opposition-Based Learning," in *Proceedings of the 2021 IEEE Congress on Evolutionary Computation (CEC)* (IEEE, 2021), 1233–1240.